

Scanning force microscopy of nanofibrillar structure of drawn polyethylene tapes

2. Measurements under water

A. Wawkuschewski¹, H.-J. Cantow¹, S. N. Magonov^{1,*}, S. S. Sheiko², and M. Möller²

¹Freiburger Materialforschungszentrum und Universität für Makromolekulare Chemie, Albert-Ludwigs-Universität, Stefan-Meier-Strasse 31 A, D-79104 Freiburg, Germany

²Organische Chemie III, Makromolekulare Chemie, Universität Ulm, Albert-Einstein-Strasse 11, D-89069 Ulm, Germany

SUMMARY

Atomic force microscopy studies of drawn ultra high molecular weight polyethylene tapes were conducted under water, where the operating repulsive forces and the contact area between probe and sample are smaller than in ambient conditions measurements. In this way a higher image resolution allows to identify nanofibrils with widths of 15-25nm, which are formed during stretching. Numerous linear features with separation of 5-8 nm were resolved on the surfaces of nanofibrils in a tape with draw ratio 70. Periodical contrast variations along the stretching direction with a repeat distance of ca. 25 nm - *long period* - were found on drawn tapes only at stronger operation forces. This finding indicates that these features are related not to the surface topography but to differences in surface hardness. From the molecular scale images it is evident that the harder parts of nanofibrils consist of crystalline domains of extended polymer chains, while no ordered features were found between the elevated image patterns.

INTRODUCTION

Atomic force microscopy (AFM), which is based on probing the repulsive interatomic force between a tiny probe and a surface, is the new technique applied to study polymer surfaces (1). First it was demonstrated that the surface morphology of crystalline polymers and amorphous block copolymers can be recorded in the AFM images (2). Then the AFM ability to reveal the periodical surface structures with the molecular resolution, which is known from studies of organic and inorganic crystals, was demonstrated also on polymer samples. Periodical molecular scale features were registered in the images of polydiacetylene single crystals, oriented polyethylene, polytetrafluoroethylene and other polymer samples (3). These images correlate well to the expected packing of surface molecular groups and extended polymer chains. It is more difficult to reliably record surface features in the scale from 1 to 100 nm because in this range the tip shape artefacts screen the actual sample morphology. This effect has limited the AFM access to nanostructure of polymers, which is responsible for many of their properties.

*Corresponding author

In the preceding paper we showed that in the experiments with selected sharp tips and in the appropriate scanning force microscopy (SFM) mode one can improve the AFM resolution and unambiguously detect the *long period* features in drawn ultrahigh molecular weight polyethylene - UHMW PE - tapes (4). Another problem of AFM applications to polymers is related to destructive surface modification, which is caused by the tip (5). To avoid this difficulty new SFM modes, such as tapping mode - TM - are developed. In the contact AFM tip-surface force interactions determine the contact area and, consequently, the image resolution. In the ambient condition experiments these forces are in the range of 10^{-7} - 10^{-9} N. At an applied force of 10^{-9} N a contact area between a ceramic tip and an organic surface was estimated as 2 nm (6). This value gives the limit of the AFM resolution in air. There is no contradiction between this result and the experimental observation of surface atomic or molecular lattices achieved in AFM. Periodical image contrast variations, which are consistent with a surface lattice, can be expected even in the case of a multiatom contact (7). Indeed, the atomic-scale defects - such as single atom vacancies - which might be regarded as indication on a one-atom contact, were not observed in AFM. In operation in air linear dislocations - at least several nm in length - are the smallest surface imperfections found in the images (8). By lowering the interacting forces and, correspondingly, by diminishing the contact area one may expect that the image resolution will be improved. This situation is realized in measurements under liquid, where the interacting forces are much lower than in air. AFM imaging in liquid becomes a routine procedure in studies of soft biological samples (9). The lateral resolution on biological objects varies in the range from 1 to 50 nm, depending on the sample. Also on hard samples the operation under liquid might be useful for the registration of local imperfections. Surface steps, separating the terraces with atomically resolved structures, and molecular vacancies within a surface lattice were recently registered in studies conducted under water (10). Thus, the measurements in liquid with selected sharp tips should provide AFM images with a better resolution. This circumstance motivated us to re-examine the surfaces of the drawn UHMW PE tapes under water. Because of the hydrophobic character of this polymer no surfaces changes occur.

EXPERIMENTAL

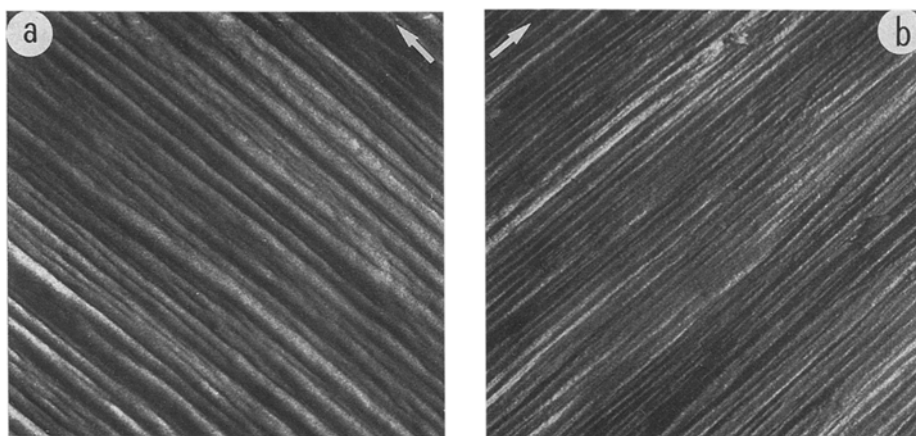
In our experiments UHMW PE tapes with draw ratio $\lambda = 10, 30$ and 70 were used. These tapes were prepared as described earlier (11). AFM studies were conducted in air and in the liquid cell, which was filled with bidistilled water. Scanning probe microscope "Nanoscope III" (Digital Instruments Inc., Santa Barbara, USA) was used in the experiments. Measurements were performed with the simultaneous registration of height, normal force (normal deflection of a cantilever) or lateral force (cantilever torsion) images, which will be

named HT, NF, LF images, respectively. In a optical lever registration scheme a laser beam, which is reflected from the back side cantilever surface, is directed to a quadrant photodetector. A differential signal of the horizontal segments is determined by the cantilever torsion and that of the vertical segments by the normal cantilever deflections. When an examined surface is flat and the geometry between a scanning direction and position of horizontal detectors is optimal (rotation angle - 90°) then the cantilever torsion is related to the variations of local friction between a probe and a surface. On corrugated surfaces of drawn PE tapes the best resolved images are recorded at a rotation angle $\pm 45^\circ$, which determines the orientation of the tape with respect to scanning directions. In such a case the response of the horizontal detectors is difficult to interpret. However, LF images, as well as NF images, provide more resolved details than HT pictures. Thus, they can be useful in surface characterization.

For the experiments we have selected those of the commercially available Si probes ("Nanoprobes") that reproduced best the vertical profile of the calibration gauge (12). This procedure allows us to choose sharp probes with an apex radius smaller than 10 nm.

RESULTS

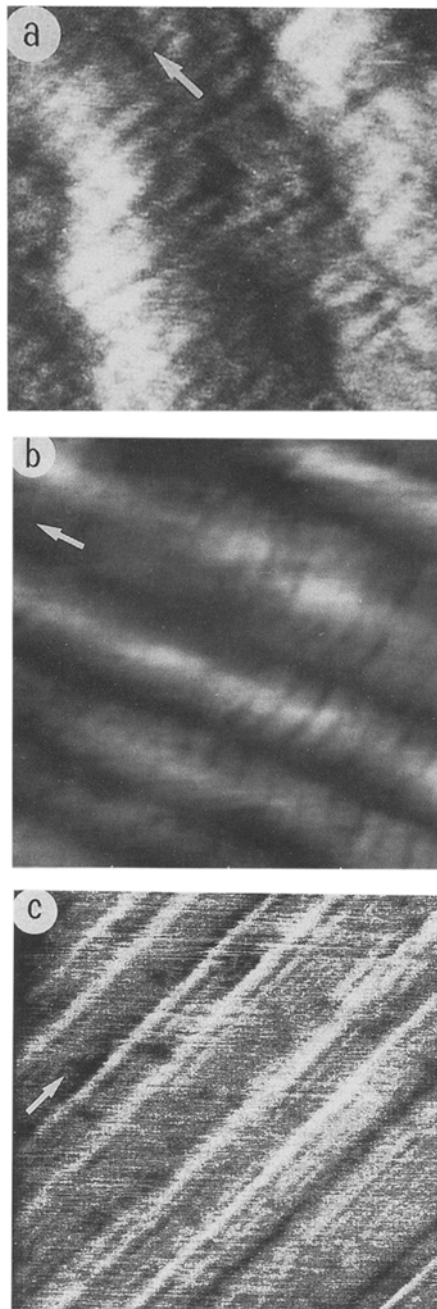
Uniaxial stretching of UHMW PE tapes is accompanied by drastic structural rearrangements, with a formation of a nanofibrillar structure. The ambient condition AFM studies of these films with selected sharp probes showed that the transverse size of such nanofibrils is 30 - 50 nm (4). A striking difference is seen between the AFM images, which were obtained on the surface of



Figures 1a - 1b: NF images of drawn UHMW PE tape ($\lambda = 70$) - (a) - in air and - (b) - in water. Stretching direction indicated by an arrow. An area of $1.69 \times 1.69 \mu\text{m}^2$ is presented in both images. A gray-scale contrast shows normal cantilever deflections within 10 nm.

highly drawn PE tape in air and in water with the same tip, Fig. 1a - 1b. The width of the linear AFM patterns recorded in water is ca. 15 - 25 nm or 2 times smaller than that of nanofibrils registered in air. These features can be assigned to individual fibrils because in some places such patterns resemble 'pull-out' or broken nanofibrils. In addition, elongated features with a width 5 - 8 nm were found on surface of nanofibrils in NF and LF images. They might be related to the surface structure of nanofibrils, and can be considered as the precursors of splitting to even smaller fibrils upon further stretching. The existence of fibers with width of 5 - 20 nm was detected in ultrahigh drawn gel-spun Spectra 900 and 1000 PE fibers with synchrotron X ray diffraction (13).

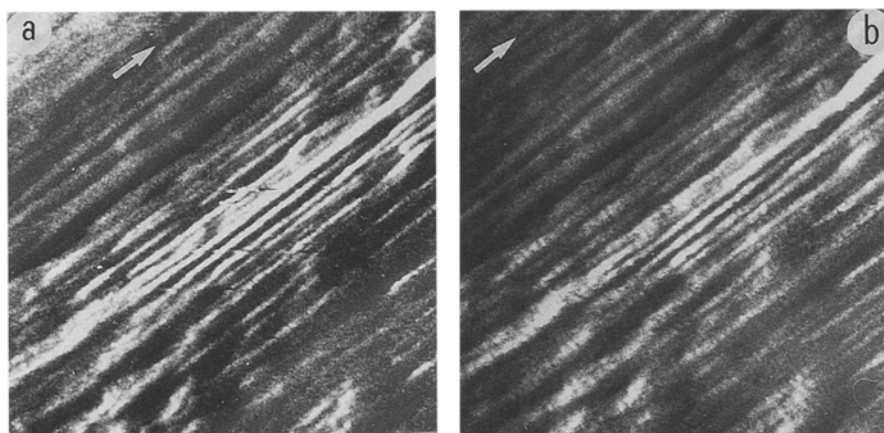
These results clearly indicate the influence of the forces between tip and sample on the image resolution. When the tip and the sample are immersed completely in a liquid, the applied force is reduced 1 - 2 orders of magnitude as compared with that in air (9a). According to the macroscopical indentation theory, the diameter of the contact zone between a ball-shape indenter and a flat surface is proportional to $p^{1/3}$, where p is the force of indentation (6). Thus, during the operation in liquid a smaller contact area is the reason of the improved resolution. Consequently, AFM images obtained in water provide the more precise dimensions of the nanofibrils in PE tapes and reveal their sub-structure.



Figures 2a - 2c: LF images of drawn UHMW PE tapes with $\lambda = 10$ - (a) - in air - $\lambda = 70$ - (b) - in air and (c) - in water. Scanning areas in all images $400 \times 400 \text{ nm}^2$. Stretching direction is indicated by arrow. The contrast in LF images indicates the variations in the differential signal of the horizontal detectors.

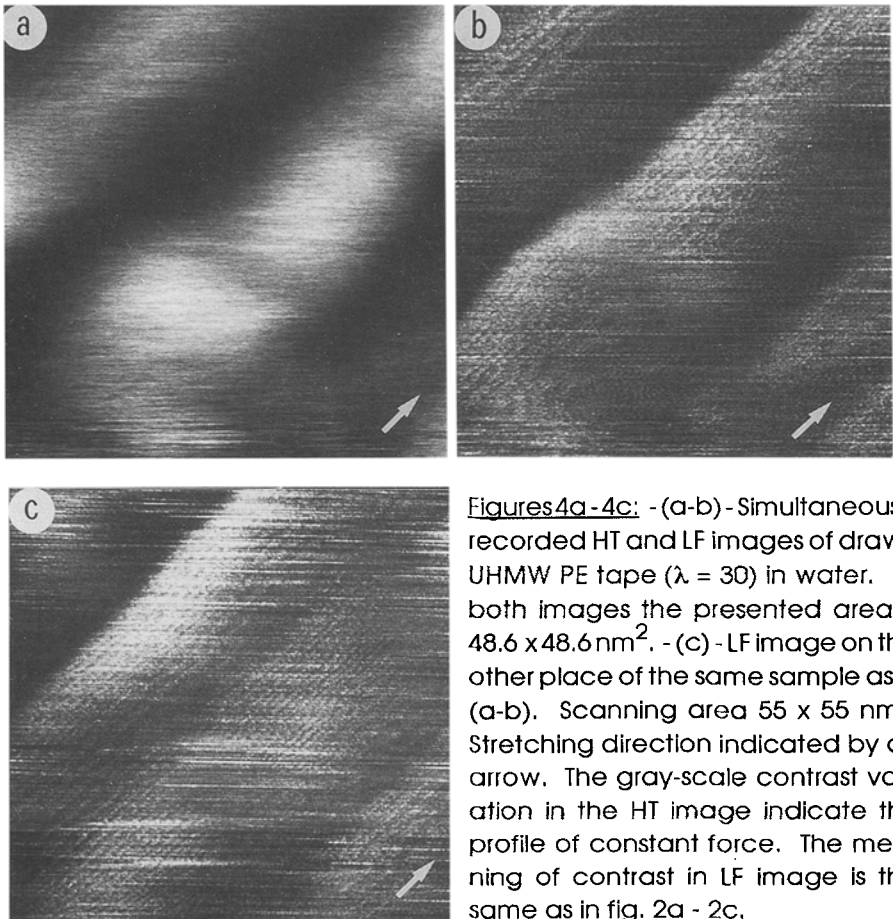
In the preceding paper (4) we showed that the periodical 'stripes' perpendicular to the stretching direction were found in the NF, LF and TM images, recorded at ambient conditions with the sharp tips, Fig. 2a - 2b. The periodicity of these contrast variations around 25 nm correlates with the *long period* values, which were found on gel-drawn UHMW PE by other techniques. These features are seen in the necked material ($\lambda = 10$), and they are distinguished on surface of nanofibrils of highly drawn tapes ($\lambda = 30, 70$). The appearance of *long period* features in the necked material may be explained by breaking off lamellae, which are lying flat within the initial tape, into blocks and their subsequent rotation. In such a way molecular chains become oriented along the stretching direction. During further drawing these blocks, which are connected by tie molecules, transform into nanofibrils (14).

In the analysis of AFM images a crucial question is related to the origin of contrast. Topography and local variations of surface hardness may be responsible for the appearance of elevated (brighter) and depressed (darker) image patterns. The measurements under water appeared to be extremely useful for a deeper understanding of the contrast variations assigned to the *long period*. First, we have observed that these variations were not always found in the images recorded in water, Fig. 2c. Then by applying different forces during imaging PE tape ($\lambda = 10$) we realized that the *long period* features appeared only after an increase of the operating force, Fig. 3a - 3b. In the measurements in air the *long period* contrast variations also increased with higher forces. The reproducibility of the results, however, was poor. These findings unambiguously indicates that the contrast variations are related to the surface regions with different local hardness but not to surface topography. Thus, the respective images might be considered as maps of nanohardness.



Figures 3a - 3b: NF images of drawn UHMW PE ($\lambda = 10$) - (a) at lower and (b) at higher force. Stretching direction indicated by an arrow. Scanning area $1.0 \times 1.0 \mu^2$. A gray-scale shows the normal cantilever deflections within 10 nm.

The relation between nanomechanical features and polymer structure was found in the molecular scale images. It is recognized that the improvement of the AFM resolution achieved in water may be useful for the detection of the molecular and atomic-scale imperfections, which are not found by experiments in air (10). Earlier only well-ordered arrays of the chain patterns with separation of 0.5 and 0.7 nm, assigned to extended polymer molecules, were found in images of cold-extruded PE (3b) and of UHMW PE tapes (11). During measurements in water the simultaneously recorded HT and LF images (Fig. 4a - 4b) show that the arrays of linear features separated by 0.5 nm are seen on the elevated spots. This observation is also confirmed by the image in Fig. 4c, where PE chains are seen on patterns separated by 25 nm; the periodical image features are absent between these patterns. This finding shows that PE crystalline domains, which are periodically arranged along nanofibrils, are the places with a higher hardness. Consequently, they are seen as the brighter AFM patterns. These crystalline domains are separated by softer amorphous regions. Thus, AFM results confirm the structural model of highly drawn polyethylene, introduced by Peterlin (14).



Figures 4a - 4c: - (a-b) - Simultaneously recorded HT and LF images of drawn UHMW PE tape ($\lambda = 30$) in water. In both images the presented area is $48.6 \times 48.6 \text{ nm}^2$. - (c) - LF image on the other place of the same sample as in (a-b). Scanning area $55 \times 55 \text{ nm}^2$. Stretching direction indicated by an arrow. The gray-scale contrast variation in the HT image indicate the profile of constant force. The meaning of contrast in LF image is the same as in fig. 2a - 2c.

CONCLUSIONS

In conclusion, the presented results demonstrate that AFM experiments under water offer the optimal conditions for a precise and unambiguous registration of surface features in nanometer scale and for their further assignment to topographical or mechanical details. In such a way the diameter of the PE nanofibrils in ultradrawn tapes was determined, and the observed *long period* features were explained by periodical variations of local hardness, associated with the crystalline domains.

REFERENCES

1. (a) Magonov SN, Cantow H-J (1992) J Appl Polym Sci, Appl Polym Symp 51:31
(b) Magonov SN (1993) Appl Spectr Rev 28:1
2. (a) Patil R, Kim S-J, Smith E, Reneker D, Weisenhorn AC (1990) Polym Comm 31:455
(b) Annis BK, Schmark DW, Reffner JR, Thomas EL, Wunderlich B (1992) Macromol Chem 193:2589
3. (a) Magonov S N, Bar G, Cantow H-J, Bauer H-D, Müller I, Schwoerer M (1991) Polym Bull 26:223
(b) Magonov S N, Qvarnström K, Elings V, Cantow H -J (1991) *ibid* 25:689
(c) Magonov S N, Kempf S, Kimmig M, Cantow H-J (1991) *ibid* 26:715
(d) Snetivy D, Guillet J E, Vansco GJ (1993) Polymer 34:429
(e) Snetivy D, Vansco G J, Rutledge GC (1992) Macromolecules 25:7037
4. Sheiko S, Möller M, Cantow H-J, Magonov SN (1993) Polym Bull, preceeding paper
5. Leung OM, Goh MC (1992) Science 255:64
6. Weihs TP, Nawaz Z, Jarvis SP, Pethica JB (1991) Appl Phys Lett 59:3536
7. Landman U, Luedke WD, Nitzan A (1989) Surf Sci Lett 10:L177
8. (a) Garnæs J, Schwarz DK, Viswanathan R, Zasadzinski JAN (1992) Nature 357:54
9. (a) Weisenhorn AL, Maivald P, Butt H-J, Hansma PK (1992) Phys Rev B45:11226
(b) Hoh J H, Hansma PK (1992) Trend Cell Biol 2:208
10. (a) Ohnesorge F, Binnig G (1993) Science 260:1451
(b) Butt H-J, Seifert E, Bamberg E (1993) J Phys Chem 97:7316
11. Magonov SN, Sheiko SS, Deblieck RAC, Möller M (1993) Macromolecules 26:1380
12. Sheiko SS, Möller M, Reuvekamp EMCM, Zandbergen HW (1993) Phys Rev B48: 5765
13. Grubb DT, Prasad K (1992) Macromolecules 25:4575
14. Peterlin A (1965) J Polym Sci C9:61